ELSEVIER

Biochimica et Biophysica Acta 1280 (1996) 207–216

BBA Biochimica et Biophysica Acta

A voltage-dependent chloride channel from *Tetrahymena* ciliary membrane incorporated into planar lipid bilayers

Chie Fujiwara-Hirashima [a], Kazunori Anzai [a,b], Mihoko Takahashi [c], Yutaka Kirino [a,d,*]

[a] *Faculty of Pharmaceutical Sciences, Kyushu University, Higashi-ku, Fukuoka 812, Japan*
[b] *National Institute of Radiological Sciences, Inage-ku, Chiba 263, Japan*
[c] *Institute of Biological Sciences, University of Tsukuba, Tsukuba, Ibaraki 305, Japan*
[d] *Faculty of Pharmaceutical Sciences, The University of Tokyo, Bunkyo-ku, Tokyo 113, Japan*

Received 11 September 1995; revised 15 November 1995; accepted 30 November 1995

Abstract

Membrane vesicles from cilia of *Tetrahymena thermophila* were incorporated into a planar phospholipid bilayer membrane, and single-channel currents across the planar membrane were recorded under voltage-clamp conditions. A novel and reproducible chloride channel was observed when a mixture of phosphatidylethanolamine and phosphatidylcholine was used to form the planar lipid membrane but not when acidic phospholipid mixtures such as asolectin or a mixture containing phosphatidylserine. Using symmetrical 100 mM KCl solutions, the single-channel conductance of the fully open state (O1) was 73.1 pS, with sub-level (O2) conductance of 9.0 pS. The permeability ratio P_{Cl}/P_K was calculated as 3.7, according to the Goldman-Hodgkin-Katz current equation. This channel exhibited characteristic voltage-dependent burst activities. With an increase in membrane potential, the lifetimes of both the burst and interburst states decreased. In the burst state, the frequency of transition between the O1 and O2 states was also voltage-dependent, mainly due to the decrease in the lifetime of the O1 state, with an increase in membrane potential. In addition, channel activity was inhibited by indanyloxyacetic acid-94 (IAA-94), an inhibitor of epithelial chloride channels.

Keywords: Chloride channel; Ciliary membrane; Voltage-dependence; Bursting activity; IAA-94; (*Tetrahymena*)

1. Introduction

Tetrahymena, a relative of *Paramecium*, is an excitable unicellular organism that generates Ca-dependent action potentials [1–3]. The putative Ca channels related to these action potentials are thought to be localized in ciliary membranes [4]. To elucidate the ionic mechanisms of membrane excitability, ion channels from *Tetrahymena* cilia have been investigated at the single-channel level. Using the planar lipid bilayer method, different types of cation channels from *Tetrahymena* cilia have been detected and characterized: voltage-independent cation channels [5–8] and voltage-dependent cation channels (Fujiwara, C. et al., unpublished data). However, the Ca channel has not yet been detected.

In attempts to detect a putative Ca channel in ciliary membrane of *Tetrahymena thermophila* by reconstituting into planar lipid membranes, we varied different experimental conditions, including the phospholipid composition of the planar lipid membrane. In the course of those experiments, we detected a novel chloride channel using a planar lipid membrane of a limited composition.

In this paper, we present the first report of a chloride channel in the ciliary membrane of ciliates. Its electrical and pharmacological properties are characterized at single-channel level.

2. Materials and methods

2.1. Preparation of ciliary membrane vesicles

Ciliary membrane vesicles of *Tetrahymena thermophila* (strain BII) were prepared as described previously [5,6] with some modifications. Cells were cultured in a medium containing 1% proteose peptone, 0.1% yeast extract, and 10 mM Mops buffer solution (adjusted to pH 7.0 with Tris; 10 mM Mops-Tris, pH 7.0) at 30°C. Cells in the late

* Corresponding author (University of Tokyo). Fax: +81 3 38146937; e-mail: kirino@mayqueen.f.u-tokyo.ac.jp.

SSDI 0005-2736(95)00292-8

logarithmic growth phase were harvested and washed with a solution of 10 mM Mops-Tris (pH 7.0) at room temperature. Cilia were detached from cell bodies by Ca^{2+}-ethanol shock according to Gibbons [9]. Cilia were washed with a solution containing 1 mM Tris and 0.1 mM EGTA (adjusted to pH 8.2 with HCl) and incubated in the same buffer for 2 h. The swollen cilia were disrupted with vigorous vortexing for 3 min, and ciliary membranes were collected by discontinuous sucrose density gradient centrifugation (20, 45, 55 and 66% sucrose) according to Adoutte et al. [10]. Ciliary membrane vesicles were sedimented as a white turbid band at the interface of the 20 and 45% sucrose layers. They were washed with a solution containing 0.3 M sucrose and 10 mM Mops-Tris (pH 7.0) and suspended in the same solution. The washed membrane vesicles were stored in liquid nitrogen until use. Purity of the cilia before the swelling procedure was assessed by electron microscopy following fixation with glutaraldehyde and staining with osmium tetroxide. No contamination by other organella was found.

2.2. Formation of planar lipid bilayers

Planar bilayers were formed by the folding method originally described by Takagi et al. [11] and modified by Montal and Mueller [12]. A Teflon chamber was separated into two compartments (*cis* and *trans*, each with an internal volume of about 1.5 ml) by a thin Teflon septum (25 μm thick) with an aperture 150–200 μm in diameter. The aperture was pretreated with a solution of 1% *n*-hexadecane in *n*-hexane before forming membranes. The solution in each compartment was connected to an Ag/AgCl electrode via a saturated KCl/agar salt bridge for current measurements under voltage-clamp conditions. A 20 μl phospholipid solution (a 7:3 (w/w) mixture of phosphatidylethanolamine (PE) and phosphatidylcholine (PC), 10 mg/ml in *n*-hexane) was placed on the surface of 0.5 ml of a 10 mM Mops buffer solution (adjusted to pH 7.0 with Tris) containing appropriate salts in each compartment. After a few minutes, the solvent evaporated and a lipid monolayer was formed at the air/water interface. The water level in each compartment was then raised by the addition of buffer solution through a syringe connected to the chamber, over the aperture, where the lipid bilayer was formed.

In most experiments, we used neutral phospholipid membranes as described above. In some experiments, we used lipid membranes with other compositions. As an acidic membrane, we used a mixture of 49% PE, 21% PC and 30% phosphatidylserine (PS) in both compartments of the chamber. As a basic membrane, we used a mixture of 49% PE, 21% PC and 30% synthetic basic lipid, 1,2-dioleoyloxy-3-(trimethylammonio)propane (DOTAP). An asymmetric membrane was made using two different membrane lipid mixtures in each compartment of the chamber. The stability of the membrane was checked applying +100 mV or −100 mV for 6 min. The membrane of which capacitance was more than 0.4 μF/cm^2 and of which conductance was less than 4 pS was used for the experiment.

2.3. Incorporation of vesicles into planar bilayers and measurement of membrane currents

A suspension of ciliary membrane vesicles was added to one compartment (*cis*) of the chamber after the membrane was formed. The final concentration of vesicles was 1–10 μg protein/ml. The holding voltage was defined as the potential of the *trans* compartment with respect to the *cis* compartment. A holding potential of −60 mV was imposed and the *cis* solution was stirred until a step increase in membrane current was detected. Channel currents were measured with a current/voltage converter (bandwidth, 1 kHz) constructed in our laboratory, and were displayed on both an oscilloscope and a chart recorder. The data were stored on a videotape after digitization using a modified digital audio processor (PCM-501ES, Sony). All experiments were carried out at room temperature (20–25°C).

2.4. Data analysis

The channel currents recorded on the videotape were transcribed on a pen oscillograph (WR3101, Graphtec, Tokyo, Japan) or a chart recorder after conditioning by an active four-pole low-pass filter (frequencies given in the figure legends). Single-channel conductance and the lifetimes of the burst period and the interburst period were analyzed by hand.

Intraburst current fluctuation was analyzed by the PAT (ver. 6.2) program (kindly provided by Dr. J. Dempster, University of Strathclyde, Glasgow, UK) on a Hewlett-Packard microcomputer after digitization at a sampling rate of 2 kHz with a 12-bit A/D converter (DT2801, Data Translation, Marlboro, MA, USA).

All single-channel analysis was performed using membranes which include one chloride channel activity with one leak-type channel activity, because the emergence of one chloride channel current was always accompanied by one leak-type channel current.

2.5. Chemicals

L-α-Phosphatidylethanolamine (PE, egg), L-α-phosphatidylcholine (PC, egg) and L-α-phosphatidylserine (PS, bovine brain) were obtained from Avanti Polar Lipids (Alabaster, AL, USA) or Nichiyu Liposome Co. (Amagasaki, Japan). 1,2-Dioleoyloxy-3-(trimethylammonio)propane (DOTAP) was synthesized as previously described [13]. Adenosine 5′-trisphosphate (ATP) was pur-

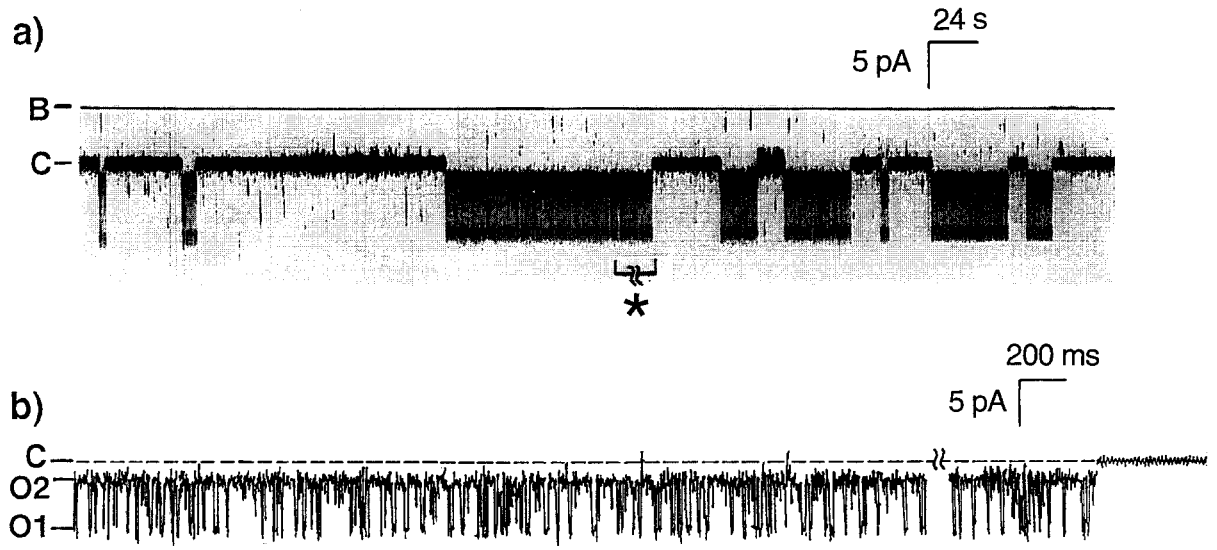

Fig. 1. Single-channel current trace recorded after incorporation of *Tetrahymena* ciliary membrane into a planar lipid bilayer in symmetrical solutions of 100 mM KCl and 10 mM Mops-Tris (pH 7.0). The composition of the planar lipid membrane was PE/PC = 7:3 (w/w) and the membrane potential (potential at the *trans* compartment with respect to the *cis* compartment) was +80 mV. 'B' indicates a current level of zero. 'C' indicates a closed level of a bursting channel current, which corresponds to an open level of a leak channel current. (a) The bursting current emerged occasionally, while the leak current remains constant conductance level (level, 'C') throughout measurement. (b) Current fluctuations, shown in an expanded time scale, of the period indicated by an asterisk in (a). During a burst, two current levels (indicated by 'O1' and 'O2') were observed. All records were filtered at 320 Hz.

chased from Wako Pure Chemical Industries (Osaka, Japan). 4,4′-Diisothiocyano-1,2-diphenylethane-2,2′-disulfonic acid (DIDS) was obtained from Nakalai Tesque (Kyoto, Japan) and indanyloxyacetic acid-94 (IAA-94; *R*(+)-((6,7-dichloro-2-cyclopentyl-2,3-dihydro-2-methyl-1-oxo-1H-inden-5-yl)oxy)acetic acid) was obtained from Research Biochemical Industries (Natick, MA, USA). All other chemicals were of reagent grades.

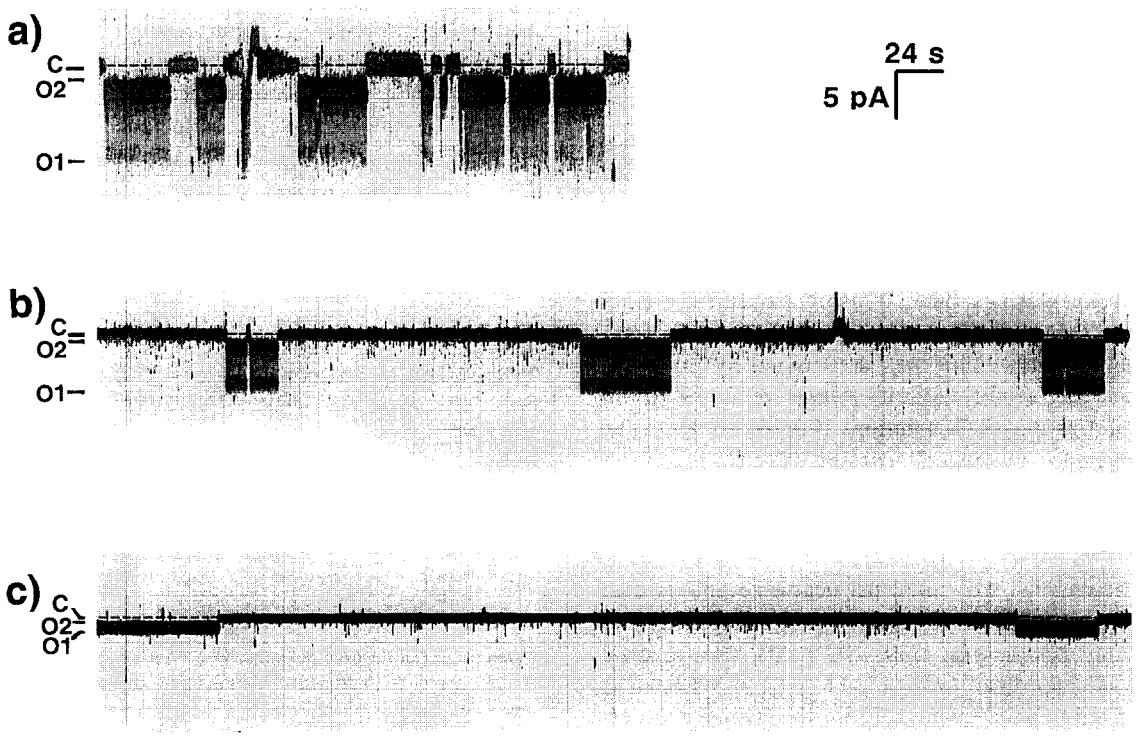

Fig. 2. Single-channel records of a chloride channel at various membrane potentials in symmetrical 100 mM KCl solutions. Burst activity was interrupted by closed periods, which we referred to as named 'interburst' (current level 'C'). O1 and O2 levels are also indicated in the traces. All records were filtered at 320 Hz. Membrane potential: (a) +100 mV; (b) +60 mV; (c) +20 mV.

3. Results

3.1. Two types of ion channels incorporated into planar bilayers

Fig. 1a shows a trace of membrane currents at +80 mV obtained after the incorporation of *Tetrahymena* ciliary membrane into the planar lipid membrane. Two types of ion channel currents were detected both frequently and reproducibly. One was a steady 'leak' current (level C in Fig. 1a and b) and the other was a 'bursting' current (levels O1 and O2 in Fig. 1b) imposed on the former. While the burst current exhibited voltage-dependent activity, as shown in Fig. 2, the leak current did not depend on membrane potential, but remained open continuously. The unit conductance of the leak current was 66 ± 15 pS (mean ± S.D., $n = 5$). The leak current was cation-selective: the reversal potential was +22.0 ± 7.5 mV (mean ± S.D., $n = 13$) in asymmetrical KCl solutions (*cis/trans*, 500/100 mM) and the permeability ratio P_{Cl}/P_K of 0.2 was deduced using the Goldman-Hodgkin-Katz current equation. The leak channel current was detected in 110 of 150 experimental runs while the burst current was found in 85 of 150. The burst current was always accompanied by the leak current. The following text focuses on the burst channel, since it is the first chloride channel detected in the ciliary membrane of ciliates.

3.2. Single-channel conductance and ion selectivity of the burst channel

The burst current exhibited bursting activities that were occasionally interrupted by silent periods, which we referred to as interburst periods (Fig. 1a, and Fig. 2). The single burst current showed three levels of conductance (Fig. 1b): fully open (O1), sub-conducting (O2) and closed (C). Since both O1 and O2 states were always detected whenever a single burst current emerged, we assumed that these two conducting states were derived from one ion channel activity. During a burst, transitions occurred mainly between the O1 and O2 states, and rarely to C state. Single-channel conductance was determined by linear regression analysis of the current–voltage relationships in symmetrical 100 mM KCl solutions (Fig. 3, circles). The slope conductance of the unit current was 73.1 ± 4.2 pS (mean ± S.D., $n = 8$) for the fully open state, O1, and 9.0 ± 1.1 pS (mean ± S.D., $n = 4$) for the sub-conducting state, O2.

The burst channel was more permeable to anions than to cations. From the current–voltage curve in asymmetrical KCl solutions (*cis/trans*, 500/100 mM), the reversal potential was determined to be −20.8 ± 1.2 mV (mean ± S.D., $n = 3$, Fig. 3, diamonds). From this value, the permeability ratio P_{Cl}/P_K was calculated to be 3.7 using the Goldman-Hodgkin-Katz current equation.

The permeabilities of various anions relative to that of

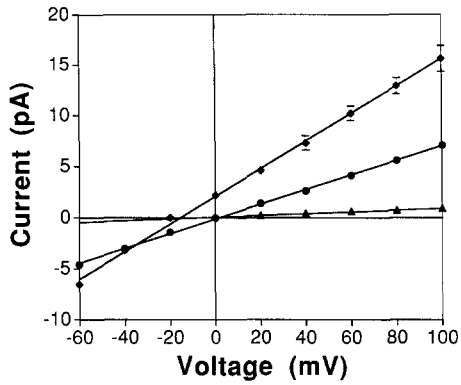

Fig. 3. Single-channel current–voltage relationship for the fully open state (O1) and partially open state (O2) of the chloride channel. In symmetrical 100 mM KCl solutions, the relationship was linear and yielded unit conductances of 73.1 ± 4.2 pS for O1 state (circles) and 9.0 ± 1.1 pS for O2 state (triangles), respectively. In asymmetrical solutions (*cis/trans*, 500/100 mM KCl; *trans* solution contained 800 mM sucrose to compensate for osmotic pressure), the current reversed at −20.8 ± 1.2 mV (diamonds). Symbols with error bars represent the mean of three or four membranes ± S.D. Small error bars are obscured by the respective symbols.

Cl^- were estimated from reversal potentials in asymmetrical solutions of 100 mM KCl in the *trans* compartment and 100 mM KBr, 100 mM KF, or 50 mM K_2SO_4 in the *cis* compartment (Table 1). The mean reversal potential for Br^- was −1.7 mV ($n = 7$), suggesting that this channel is slightly more permeable to Br^- than to Cl^-. The permeability ratio P_{Br}/P_{Cl} was calculated to be 1.1. The mean reversal potentials for F^- and SO_4^{2-} were +11.9 ($n = 7$) and +18.5 mV ($n = 2$), respectively, indicating that they are less permeant than Cl^-. The permeability ratios, P_F/P_{Cl} and P_{SO4}/P_{Cl} were calculated to be 0.52 and 0.25, respectively. The single-channel conductance for Br^- was 67.3 ± 4.8 pS (mean ± S.D., $n = 7$), which is similar to that for Cl^-. The single channel conductances for F^- and SO_4^{2-} were 52.7 ± 5.9 pS (mean ± S.D., $n = 7$) and 50.9 pS (mean, $n = 2$), respectively. Also conductance ratios were

Table 1
Single-channel conductances (g) [a], reversal potentials (V_{rev}), conductance ratios ($g_{an}{}^b/g_{Cl}$) and permeability ratios ($P_{an}{}^b/P_{Cl}$) [c] for various anions

Anion	g (pS)	V_{rev} (mV)	g_{an}/g_{Cl}	P_{an}/P_{Cl}	
Cl^-	73.1 ± 4.2	–	(1)	(1)	$n = 8$
Br^-	67.3 ± 4.8	−1.7 ± 1.0	0.92 ± 0.07	1.1 ± 0.1	$n = 7$
F^-	52.7 ± 5.9	+11.9 ± 3.4	0.72 ± 0.08	0.52 ± 0.08	$n = 7$
SO_4^{2-}	49.7	+19.4	0.68	0.23	
	52.0	+17.6	0.71	0.27	

[a] Determined at positive potential, where the current carrier (from the *cis* to the *trans* compartment) was thought to be an anion, by linear regression analysis of the current–voltage curve.
[b] 'an' refers to 'anion'.
[c] Estimated from reversal potentials in asymmetrical solutions as follows; 100 mM KCl in the *trans* compartment and 100 mM KBr, KF, or 50 mM K_2SO_4 in the *cis* compartment.

calculated (Table 1). The sequence of permeability ratios for the *Tetrahymena* chloride channel Br^- (1.1) $\geq Cl^-$ (1.0) > F^- (0.52) > SO_4^{2-} (0.25), was almost same as that of conductance ratios, Cl^- (1.0) > Br^- (0.92) > F^- (0.72) $\geq SO_4^{2-}$ (0.70).

3.3. Voltage-dependence of the lifetimes of the burst and interburst

Fig. 2 shows three current traces at different membrane potentials (+100, +60 and +20 mV from up to bottom). The lifetime of the interburst state (closed state, C) was dramatically reduced as the membrane potential increased. The lifetime of the burst state (O1 and O2 state) was also voltage-dependent. Fig. 4 shows the lifetime histograms of the burst (a) and interburst (b) from four membranes. Both histograms, especially that for the interburst, showed longer lifetimes as the membrane potential decreased. At less than −20 mV, the frequency of the channel current appearance was quite low. Bursting probability (P_B) was calculated using the following equation:

$$P_B = \Sigma T_B / (\Sigma T_B + \Sigma T_{IB}) \quad (1)$$

where T_B and T_{IB} indicate individual burst and interburst lifetimes, respectively. P_B is plotted against membrane potential in Fig. 5. Mean bursting probability increased as the membrane potential increased. The mean bursting probability ± S.D. from four membranes at +20 mV and +100 mV was 0.22 ± 0.29 and 0.66 ± 0.34 (mean ± S.D., $n = 4$), respectively. Accordingly, 80 mV increase in membrane potential causes 3-fold increase in P_B. This implies that bursting probability rather weakly depends on membrane potential.

3.4. Voltage-dependence of intraburst events

During a burst period, the current transition between O1 and O2 was also voltage-dependent. Fig. 6 shows four current traces at membrane potentials of +100, +80, +60 and +40 mV from up to bottom. The lifetime of the O1 state increased as the membrane potential decreased. The intraburst current was analyzed using the single-channel current analyzing computer program, PAT [14]. The amplitude histogram of the current was composed of two peaks, as shown in Fig. 7a: the left peak indicates O2-state current, and the right peak indicates O1-state current. These peaks were best-fitted by a Gaussian function, and the area under the Gaussian curve was determined. The probability of remaining at O1 (P_{O1}) was calculated from Eq. (2),

$$P_{O1} = A_{O1} / (A_{O1} + A_{O2}) \quad (2)$$

where A_{O1} and A_{O2} indicate the corresponding peak areas in Fig. 7a. Fig. 7b shows P_{O1} as a function of membrane potential. P_{O1} decreased monotonically as the membrane potential increased.

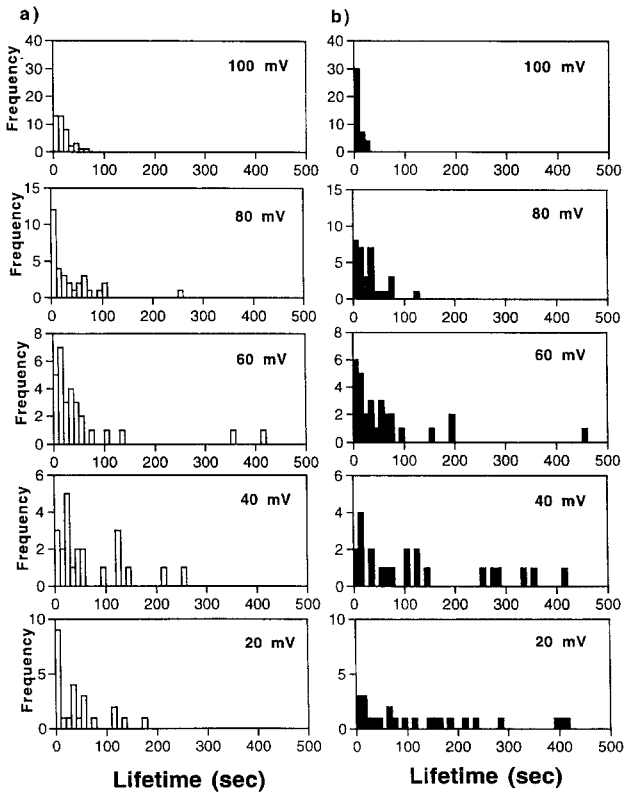

Fig. 4. Lifetime histograms of burst (a) and interburst (b) in symmetrical 100 mM KCl solutions at the membrane potentials indicated. The burst and interburst events were counted for 10 s bins. Each histogram was constructed from the data from four membranes.

Lifetime histograms of O1 and O2 within a burst at +60 mV are shown in Fig. 8. Each histogram was well fitted with a single exponential function. This implies that each level of current is associated with a single state. The mean lifetime of the O1 and O2 states, which is equal to the reciprocal of the decay time constant for O1 and O2, respectively, is plotted as a function of membrane potential in Fig. 9. The mean lifetime of the O1 state (Fig. 9a) decreased as the membrane potential increased, while that of the O2 state (Fig. 9b) did not show any definite voltage-dependency. This suggests that the voltage-dependence of the transition between O1 and O2 is due to the voltage-dependence of the lifetime of the O1 state.

3.5. Pharmacology

Several channel blockers were tested. ATP (5 mM), which blocks the anion channel in human platelet plasma membrane [15], did not block the present chloride channel current when it was added to either the *cis* or *trans* compartment. The effect of DIDS, which has been widely used as a specific inhibitor of various anion channels [16,17], was complex. In most of the experiments (8 of 11), 5 μM of DIDS irregularly increased cationic membrane currents, while in the other experiments (3 of 11) it

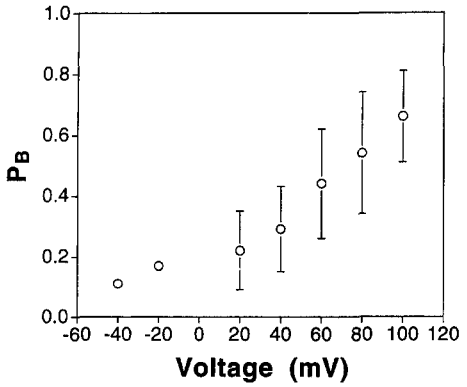

Fig. 5. Voltage-dependence of bursting probability (P_B). P_B was calculated from Eq. 1 in the text. Symbol with error bar represents the mean of four membranes ± S.D. The data at −20 and −40 mV were from a single membrane. The total number of burst and interburst events at each voltage was 44–88, except at −20 and −40 mV. At −20 and −40 mV, P_B was obtained from 10-min records in which 4 (at −20 mV) or 2 (at −40 mV) burst and interburst events were observed.

decreased both the leak and the chloride channel currents. Both effects were irreversible: perfusion of the chamber with a standard buffer solution to remove DIDS failed to restore the original currents.

Fig. 10 shows the effect of IAA-94, a polycyclic compound which is a potent inhibitor of tracheal and kidney epithelial chloride transport [18]. The addition of 588 μM IAA-94 to the *trans* compartment decreased the single-channel conductance to 70% of the control (Fig. 10b), and

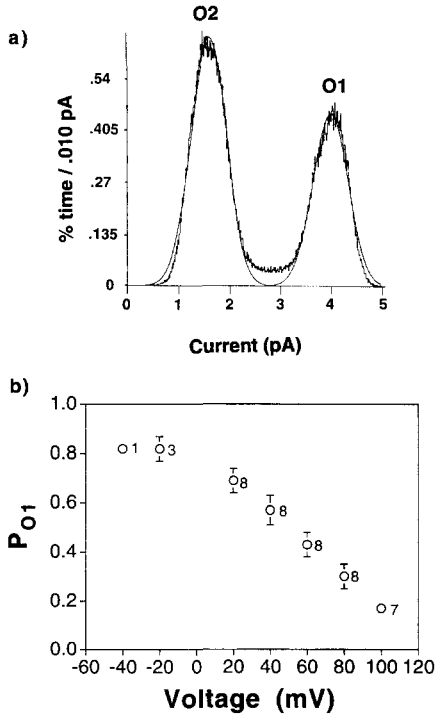

Fig. 7. (a) Amplitude histogram of burst current at +40 mV. This histogram was constructed from more than 4800 events over 90 s. The percentage of total sampling time was calculated for 0.01 pA bins. The peak-fitted line indicates the best-fit Gaussian curve for the peak. (b) The voltage-dependence of probability of being in state O1 (P_{O1}). P_{O1} was calculated from Eq. 2 in the text. The values next to the symbols indicate the number of different membranes from which data were obtained.

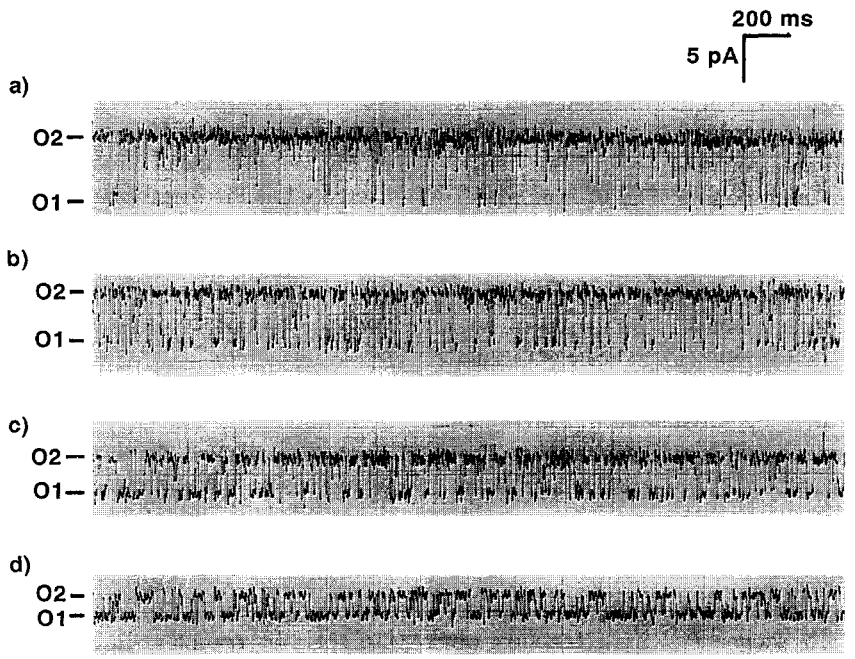

Fig. 6. Single-channel current fluctuations during a burst at various membrane voltages in symmetrical 100 mM KCl solutions. Records were filtered at 320 Hz. Membrane potential: (a) +100 mV; (b) +80 mV; (c) +60 mV; (d) +40 mV.

increased the lifetime of the O1 state, although no significant change was observed in bursting probability (Fig. 10b). When 588 μM of IAA-94 was added to both the *cis* and *trans* compartments, the lifetimes of the burst and the O1 state decreased simultaneously (Fig. 10c). The addition of IAA-94 to only the *cis* compartment affected the lifetimes of the burst and the O1 state with inhibitory effect. This inhibition was reversible: perfusion with a buffer without IAA-94 restored the channel activity (Fig. 10d).

3.6. Effect of membrane phospholipid composition

When we used asolectin (soybean phospholipid) to form planar membranes in previous studies [5,8], we detected cation channel activities reproducibly, but not the chloride channel activity described in the present study. While asolectin contains about 20% acidic phospholipid (PC, 42 mol%; PE, 39%; phosphatidic acid, 19%), the phospholipid used in the present study is neutral (PE, 70%; PC, 30%). Since the charge of the polar head group of phospholipids in the planar lipid membrane may contribute to the activity of a specific ion channel, we tested other membrane compositions (Table 2): i.e., an acidic PE/PC/phosphatidylserine (PS) (49:21:30, w/w), and a basic PE/PC/DOTAP (49:21:30, w/w).

With all the membrane compositions studied, voltage-independent leak type currents were detected very frequently. Although it is not obvious whether or not the leak currents are independent of the lipid composition, we used the appearance of leak currents as an index of the vesicle fusion to a planar lipid membrane because the chloride channel activity was always accompanied by the leak current. Accordingly, the detection ratio of the chloride channel current based on the detection of leak currents was calculated. When acidic membranes were used, the chloride channel activity was not detected at all (0/6). In contrast, the chloride channel activity was frequently observed with basic membranes (5/6). The detection ratio was very similar to that obtained with neutral membranes (85/110). We failed to detect the chloride channel activity with an asymmetrical lipid bilayer (0/3), which had a neutral monolayer on the *cis* side and an acidic monolayer on the *trans* side.

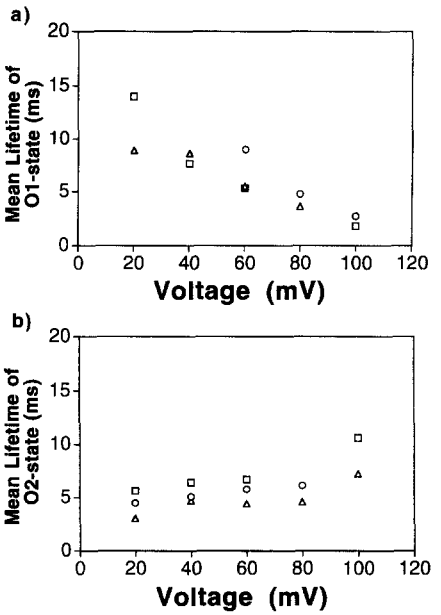

Fig. 9. Mean lifetime of O1 (a) and O2 (b) states obtained from the single exponential functions fitted to the data (Fig. 8). Different symbols represent data from different membranes.

4. Discussion

In this study, we characterized a single chloride channel current from ciliary membranes of *Tetrahymena*. The single-channel conductance was 73 pS with a sub-conducting level of 9 pS in symmetrical 100 mM KCl solutions. The unit channel current showed voltage-dependent bursting activity, and was selective to anions over cations and sensitive to IAA-94. There have been several recent devel-

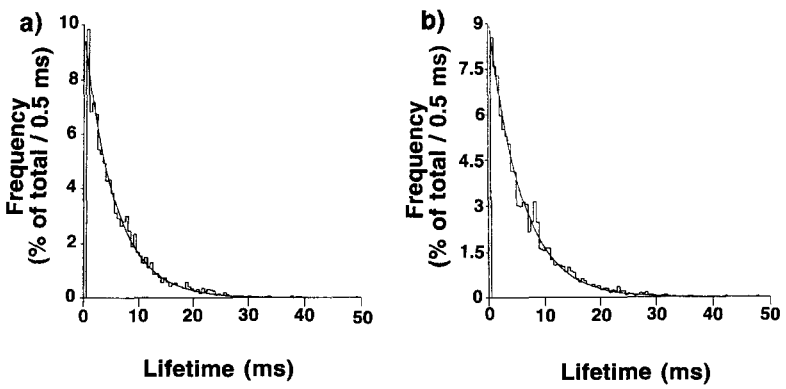

Fig. 8. Lifetime histograms of the O1 (a) and O2 (b) states. The histograms were obtained from 60 s of records of the chloride channel current at +60 mV after filtration at 320 Hz. The percentage of total events was calculated for 0.5 ms bins. A single exponential function (solid line) was well fitted to the data.

Table 2
Membrane lipid compositions and detection ratio of the anion channel activity

	Composition (w/w)	Detection ratio [a]
Symmetrical	neutral (PE/PC 7:3)	85/110
	acidic (PE/PC/PS 49:21:30)	0/6
	basic (PE/PC/DOTAP 49:21:30)	5/6
Asymmetrical [b]	*cis*, neutral; *trans*, acidic	0/3

[a] Detection ratio was calculated as follows: (detection frequency of the anion channel current)/(detection frequency of leak channel currents).
[b] The phospholipid composition of each monolayer is as described above.

opments in the study of chloride channels. Elucidating the mechanism of Cl^- transport is becoming increasingly important in understanding the function of various cells [19,20]. Based on functional properties such as gating, conductance, ion selectivity, kinetics and sensitivity to blockers, Franciolini and Petris [21] have classified chloride channels of animal cells into four categories: (1) background chloride channels that show a significant open probability at resting membrane potentials, (2) double-barreled chloride channels that exhibit characteristic gating behavior, (3) maxi chloride channels, so-named for their very high conductance, and (4) ligand-activated chloride channels, which are activated by various low molecular weight ligands, including Ca ions and neurotransmitters. In the light of these data, the single-channel conductance of 73 pS is too low for it to be considered a maxi chloride channel, but it is within the range (10–100 pS) seen for background chloride channel. Although the *Tetrahymena* chloride channel has a sub-conducting state, it is not half the full conductance, such as in double-barreled chloride channels. Furthermore, the *Tetrahymena* chloride channel does not need any ligands to be activated. If this classification is applied, the *Tetrahymena* chloride channel described in the present study belongs to background chloride channels.

4.1. Ion selectivity

Previous investigators [22] reported that the background chloride channel shows low ion-selectivity and is permeable to cations to some extent. The permeability ratio P_{Cl}/P_K of the *Tetrahymena* chloride channel current is 3.7, which is similar to the values reported for various other background chloride channels: 5–6.7 for cultured rat skeletal muscle [23], 4 for rat hippocampal neuron [24], and 3.3 for T84 human colonic cell [25].

Various anion selectivity sequences have been reported

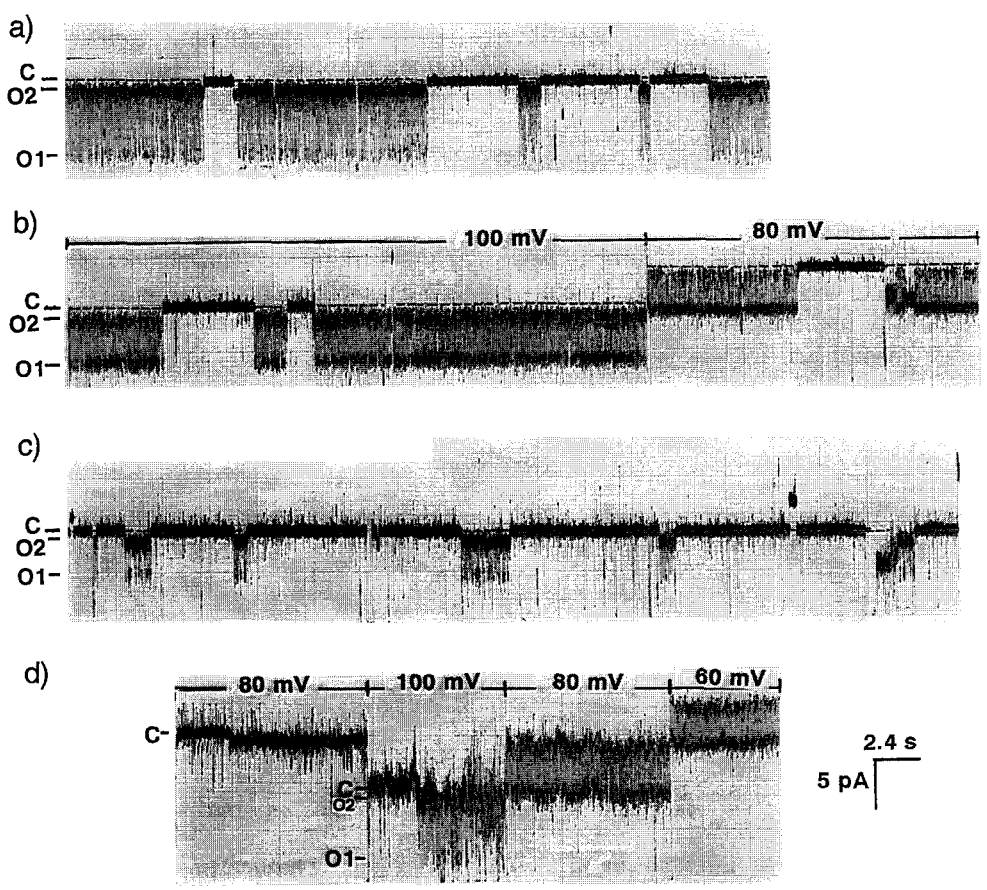

Fig. 10. Blockade of the chloride channel with IAA-94. (a) Control. (b) 588 μM IAA-94 was added to the *trans* compartment. (c) 588 μM IAA-94 was added to both the *cis* and *trans* compartments. (d) After perfusion with a buffer without IAA-94, channel activity was recovered from the membrane used for the experiment in (c). In all records, O1, O2 and closed current levels were indicated by 'O1', 'O2' and 'C', respectively.

for various other background chloride channels [20,26,27]. Most of these other channels are clearly more permeable to Br^- than to Cl^-, whereas the *Tetrahymena* chloride channel is almost equally permeable to Br^- and Cl^-. The sequence of permeability ratios for the *Tetrahymena* chloride channel current in the present study, Br^- (1.1) ≥ Cl^- (1.0) > F^- (0.52) > SO_4^{2-} (0.25), As shown in Table 1, the sequence of permeability ratios for the *Tetrahymena* chloride channel current was almost the same as that of conductance ratios. It indicates that the movement of an anion in the channel is independent of other ions during permeation [28]. The permeability ratios for *Tetrahymena* chloride channel is similar to that for the background chloride channel from rabbit urinary bladder, $Br^- = Cl^-$ (1.0) > F^- (0.5) [29].

4.2. Pharmacological characteristics

Several drugs have been used to characterize background chloride channels. Although the pharmacology for the background chloride channel is not yet fully determined, some drugs have been effective in blocking several background chloride channel activities. In this study, three blockers were tested: DIDS, ATP and IAA-94. DIDS, which is widely used as a classical chloride channel blocker, has been reported to block background chloride channel currents from muscle [16], epithelia [17,26], and neurons [30]. However, because of its complex modification of the membrane current in this study, we could not clarify the inhibitory effect of DIDS on the *Tetrahymena* chloride channel activity. Most of our experimental results with DIDS suggest that there is a novel type of cation channel in ciliary membrane from *Tetrahymena* that can be activated by DIDS. Some investigators have found that DIDS can indeed open some cation channels: K^+ channel in squid giant axon [31], K^+ channel in the vacuolar membrane of yeast [32] and the ryanodine-sensitive Ca channel from sarcoplasmic reticulum [33]. ATP has been reported almost completely to block a background-type chloride channel activity from platelet plasma membrane at 5 mM [15], and almost completely to block a calcium-dependent chloride channel activity from sheep tracheal epithelium at 100 μM [34]. However, ATP (5 mM) did not block the *Tetrahymena* channel activity in this study.

IAA-94 was the only effective blocker of the *Tetrahymena* chloride channel current. Landry et al. [35] reported that IAA-94 blocked chloride transport in vesicles isolated from bovine kidney cortex more potently than about one hundred other compounds, with an inhibition constant of 1 μM. Garber [36] reported that application of 200 μM IAA-94 to the intracellular face of outwardly rectifying chloride channel current from Jurkat lymphocytes resulted in an increase in the appearance of fast-closing events during long-open events. Grygorczyk and Bridges [29] reported that IAA-94 blocked Cl^- conductance (50% inhibition at 50 μM) in cultured cells of brushed human nasal epithelia. This conductance was blocked completely with 2.8 mM IAA-94.

In our experiments, the application of 60 μM IAA-94 to the *cis* compartment produced a slight decrease in single-channel conductance (to 95%), but did not affect bursting probability. The application of 600 μM IAA-94 produced a clear decrease in the burst lifetime. The effective concentration range for the *Tetrahymena* chloride channel was higher than that reported by Landry et al. [35], but was similar to that reported by Garber [36] or Grygorczyk and Bridges [30].

4.3. Voltage-dependence

Generally, the voltage-dependence of ion channel currents is believed to be due to a voltage-dependent change in the open probability [37]. The origin of the voltage-dependence of the *Tetrahymena* chloride channel activity was complex. The *Tetrahymena* chloride channel current shows two types of voltage-dependent transition: one is the slow (less frequent) burst-interburst transition, and the other is the faster (more frequent) transition between the O1 and O2 states within the burst. In the former, a decrease in the membrane potential decreases the bursting probability, which contributes to a decrease in the mean conductance. In the latter, however, a decrease in the membrane potential increases the probability of staying in the O1 state, which contributes to an increase in the mean conductance within a burst period. The overall mean conductance, $G_{AVERAGE}$, is calculated as:

$$G_{AVERAGE} = 73P_B P_{O1} + 9P_B(1 - P_{O1}) \quad (3)$$

The result is shown in Fig. 11, which indicates that the overall conductance of the *Tetrahymena* chloride channel shows little voltage-dependency. Since weak voltage-dependence seems characteristic of background chloride channels [20], the *Tetrahymena* chloride channel is again very likely to belong to this group. However, it is not clear whether or not the *Tetrahymena* chloride channel is indeed open at resting potential in vivo.

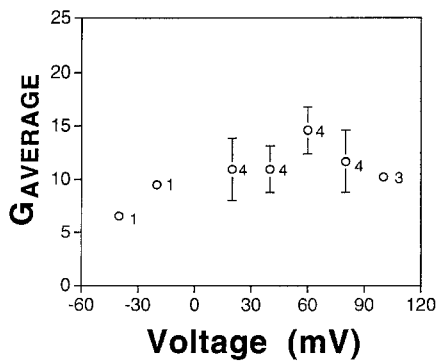

Fig. 11. Voltage-dependence of the mean overall conductance ($G_{AVERAGE}$) of the chloride channel. $G_{AVERAGE}$ was calculated from Eq. 3 in the text. Symbol with error bar represents the mean ± S.D. and the number adjacent to the symbol indicates the number of different membranes tested.

4.4. Effect of planar lipid membrane composition

The detection ratio of the *Tetrahymena* chloride channel activity strongly depended on the lipid composition of the planar membrane. The chloride channel did not show any activity with acidic asolectin membranes. In contrast, it exhibited activity frequently with the neutral PE/PC (7:3) membrane. A negative charge on the polar head groups of lipid molecules seems to contribute to the failure to detect the chloride channel current (Table 2). We failed to detect chloride channel activity with an acidic membrane (a mixture of PE/PC/PS), but did detect it with both basic and neutral membranes. Interestingly, the lipid of ciliary membrane of *Tetrahymena* is composed mostly (about 90%) of neutral lipids (e.g., Tetrahymanol) and phospholipids [38].

Previous investigators [39,40] reported the mechanism of the effect of phospholipid charge on channel activity: the lipid charge may affect the permeant ion concentrations at the mouth of the ion channel and, hence, single-channel conductance. However, this cannot explain the present result, since the lipid charge did not affect single-channel conductance of the chloride channel. Although the surface charge may change the voltage-dependence of the ion channel, it should make no difference with symmetrical lipid membranes. Another possible explanation is that different types of ciliary membrane vesicles fuse to planar membranes of different compositions. However, this is not likely since an asymmetrical membrane that had a neutral phospholipid monolayer on its *cis* side and an acidic phospholipid monolayer on its *trans* side failed to produce a detectable chloride channel activity. This result suggests that chloride channel activity is inhibited by the presence of acidic phospholipid in the *trans* monolayer, after the incorporation of the channel into the planar lipid membrane. A similar result has been recently reported [41] with the K^+ channel of sarcoplasmic reticulum that the phospholipid composition of the *trans* monolayer may affect the conformation of an ion channel protein. These results suggest that there may exist a novel type of ion channel regulation by the composition of biological membranes. Further study is needed to confirm this hypothesis.

Acknowledgements

We are very grateful to Dr. J. Dempster for kindly providing his computer program, PAT (ver. 6.2) for the single-channel current analysis. Dr. N. Hirashima is also thanked for helpful discussions.

References

[1] Connolly, J.G. and Kerkut, G.A. (1981) Comp. Biochem. Physiol. 69c, 265–273.
[2] Onimaru, H., Ohki, K., Nozawa, Y. and Naitoh, Y. (1980) Proc. Jpn. Acad. 56B, 538–543.
[3] Takahashi, M., Onimaru, H. and Naitoh, Y. (1980) Proc. Jpn. Acad. 56B, 585–590.
[4] Schultz, J.E., Schoenfeld, U. and Klumpp, S. (1983) Eur. J. Biochem. 137, 89–94.
[5] Kawahara, S., Kirino, Y., Nagao, S. and Nozawa, M. (1986) J. Biochem. 100, 1569–1573.
[6] Oosawa, Y. and Sokabe, M. (1985) Am. J. Physiol. 249, C177–179.
[7] Oosawa, Y., Sokabe, M. and Kasai, M. (1988) Cell Struct. Func. 13, 51–60.
[8] Fujiwara, C., Anzai, K., Kirino, Y., Nagao, S., Nozawa, Y. and-Takahashi, M. (1988) J. Biochem. 104, 344–348.
[9] Gibbons, I.R. (1965) Arch. Biol. (Liege) 76, 317–352.
[10] Adoutte, A., Ramanathan, R., Lewis, R.M., Dute, R.R., Ling, K.Y., Kung and C., Nelson, D.L. (1980) J. Cell Biol. 84, 717–738.
[11] Takagi, M., Azuma, K. and Kishimoto, U. (1965) Annu. Rep. Biol. Work. Fac. Sci. Osaka Univ. 13, 107–110.
[12] Montal, M. and Mueller, P. (1972) Proc. Natl. Acad. Sci. USA. 69, 3561–3566.
[13] Anzai, K., Masumi, M., Kawasaki, K. and Kirino, Y. (1993) J. Biochem. 114, 487–491.
[14] Dempster, J. (1993) Computer Analysis of Electrophysiological Signals, Academic Press, San Diego.
[15] Manning, S.D. and Williams, A.J. (1989) J. Membr. Biol. 109, 113–122.
[16] Bretag, A.H. (1987) Physiol. Rev. 67, 618–724.
[17] Greger, R. (1990) Methods Enzymol. 191, 793–810.
[18] Landry, D.W., Akabas, M.H., Redhead, C., Edelman, A., Cragoe, E.J. Jr. and Al-Awqati, Q. (1989) Science 244, 1469–1472.
[19] Alvarez-Leefmans, F.J., Giraldez, F. and Russell, J.M. (1990) in Chloride Channels and Carriers in Nerve, Muscle and Glial Cells (Alvarez-Leefmans,.F.J. and Russell, J.M., eds.), pp. 3–66, Plenum Press, New York.
[20] Frizzel, R.A. (1987) Trends Neurosci. 10, 190–193.
[21] Franciolini, F. and Petris, A. (1990) Biochim. Biophys. Acta 1031, 247–259.
[22] Franciolini, F. and Petris, A. (1992) Biochim. Biophys. Acta 1113, 1–11.
[23] Blatz, A.L. and Magleby, K.L. (1985) Biophys. J. 47, 119–123.
[24] Franciolini, F. and Nonner, W. (1987) J. Gen. Physiol. 90, 453–478.
[25] Vaca, L. and Kunze, D.L. (1992) J. Membr. Biol. 130, 241–249.
[26] Goegelein, H. (1988) Biochim. Biophys. Acta 947, 521–547.
[27] Gray, M.A., Pollard, C.E., Harris, A., Coleman, L., Greenwell, J.R. and Argent, B.E. (1990) Am. J. Physiol. 259, C752–C761.
[28] Hille, B. (1992) in Ionic Channels from Excitable Membranes (second edition) pp. 362–389, Sinauer Associates Inc., Sunderland.
[29] Grygorczyk, R. and Bridges, M.A. (1992) Can. J. Physiol. Pharmacol. 70, 1134–1141.
[30] Nomura, K. and Sokabe, M. (1991) J. Membr. Biol. 124, 53–62.
[31] Inoue, I. (1986) J. Gen. Physiol. 88, 507–520.
[32] Tanifuji, M., Sato, M., Wada, Y., Anraku, Y. and Kasai, M. (1988) J. Membr. Biol. 106, 47–55.
[33] Kawasaki, T. and Kasai, M. (1989) J. Biochem. 106, 401–405.
[34] Alton, E.W.F.W., Manning, S.D., Schlatter, P.J., Geddes, D.M. and Williams, A.J. (1991) J. Physiol. 443,137–159.
[35] Landry, D.W., Reitman, M., Cragoe, E.J. Jr. and Al-Awqati, Q. (1987) J. Gen. Physiol. 90, 779–798.
[36] Garber, S.S. (1992) J. Membr. Biol. 127, 49–56.
[37] Hille, B. (1992) in Ionic Channels from Excitable Membranes (second edition) pp. 23–58, Sinauer Associates Inc., Sunderland.
[38] Thompson, G.A.Jr. and Nozawa, Y. (1977) Biochim. Biophys. Acta 472, 55–92.
[39] Bell, J.E. and Miller, C. (1984) Biophys. J. 45, 279–287.
[40] Moczydlowski, E., Alzarez, O., Vergara, C. and Latorre, R. (1985) J. Membr. Biol. 83, 273–282.
[41] Anzai, K., Takano, C., Tanaka, K. and Kirino, Y. (1994) Biochem. Biophys. Res. Commun. 199, 1081–1087.